Chapter 1

INTRODUCTION: ALKYL-TERMINATED SILICON SURFACES

Plymale, N. T.; Kim, Y.-G.; Soriaga, M. P.; Brunschwig, B. S.; Lewis, N. S. Synthesis, Characterization, and Reactivity of Ethynyl- and Propynyl-Terminated Si(111) Surfaces. *J. Phys. Chem. C* **2015**, *119*, 19847–19862. DOI: 10.1021/acs.jpcc.5b05028

1.1 HYDROGEN-TERMINATED SILICON SURFACES

Hydrogen-terminated Si (Si–H) is the fundamental surface termination on which the vast majority of surface modification is based.[1-4] The semiconductor industry relies on the production of Si–H surfaces in order to produce high-quality silicon oxide films with low electrical defect density. Consequently, the Si–H surface has been widely studied and characterized. Si–H surfaces can be prepared by a number of techniques, including cleavage of Si in vacuum followed by exposure to H_2(g),[5] electrochemical etching,[6-9] or wet-chemical etching in aqueous fluoride solutions.[10-12] Wet-chemical etching of Si is the simplest method to produce Si–H surfaces, resulting in widespread use of this technique to produce Si–H surfaces.

Early reports of Si–H surfaces prepared by exposure of oxide-terminated Si to aqueous HF solutions suggested that the surface was terminated by Si–F bonds.[13] The basis for this initial conclusion is the known strength of the Si–F bond, which was hypothesized to form the dominant surface termination after fluoride etching based on thermodynamic arguments. However, the kinetics of the fluoride etching of Si surfaces dominates the

thermodynamics in this case; as the atop Si atoms are fluorinated, they are removed from the surface quickly because the kinetics of the cleavage of Si–Si bonds by HF drives the removal of fluorinated surface sites. The result is a surface that is free of detectable Si–F containing species. This was first demonstrated by surface infrared (IR) spectroscopy, which was used to show the presence of Si–H stretching and bending peaks on the surface.[11, 14] Vibrational spectroscopy remains a very powerful surface analytical tool, particularly when used together with other surface sensitive techniques such as X-ray photoelectron spectroscopy, because it can inform functional group assignments as well as the orientation of bonds on the surface.

HF etching of Si can be performed on any crystal face, including amorphous Si, nanocrystalline Si, or microstructured Si substrates to yield H-terminated surfaces. When etched with unbuffered HF(aq) solutions, Si surfaces are terminated by a distribution of monohydride (SiH), dihydride (SiH_2) and trihydride (SiH_3) surface sites. By adjusting the pH of the HF(aq) solution by addition of NH_4F solution, the etch rate can be controlled in order to select for the desired surface termination.[14] Anisotropic etching the (111) crystal face of silicon in 40% NH_4F(aq) solutions allows for exceptional control over the surface hydride composition, yielding primarily the monohydride H–Si(111) surface.[15] H–Si(111) is known to exhibit broad atomic terraces with >100 nm width and nearly every Si–H bond is oriented perpendicular to the surface. H–Si(111) is an extremely convenient starting surface for studying the surface chemistry of silicon because modification of H–Si(111) with halogens or organic groups results in substitution of the Si–H bonds for Si–X (X = Cl, Br, I), Si–C , or Si–O bonds. Spectroscopic methods allow for the loss of Si–H bonds to be observed, and the nature of the new bonds formed on the surface can be more readily

studied because of the inherent nature of the Si(111) surface, which has reactive Si bonds that are oriented perpendicular to the surface.

Transmission infrared spectroscopy (TIRS) was the primary vibrational spectroscopic method used throughout this work. Compared with attenuated total reflectance infrared (ATR-IR) spectroscopy, TIRS is more effective at observing low energy modes (<1500 cm^{-1}), including Si–C stretching and C–H bending modes.[15] TIRS can readily observe the orientation of bonds with respect to the sample surface by modifying the angle of incidence on the surface. Figure 1.1 shows TIRS data for a H–Si(111) surface to demonstrate its utility as a surface analytical tool.

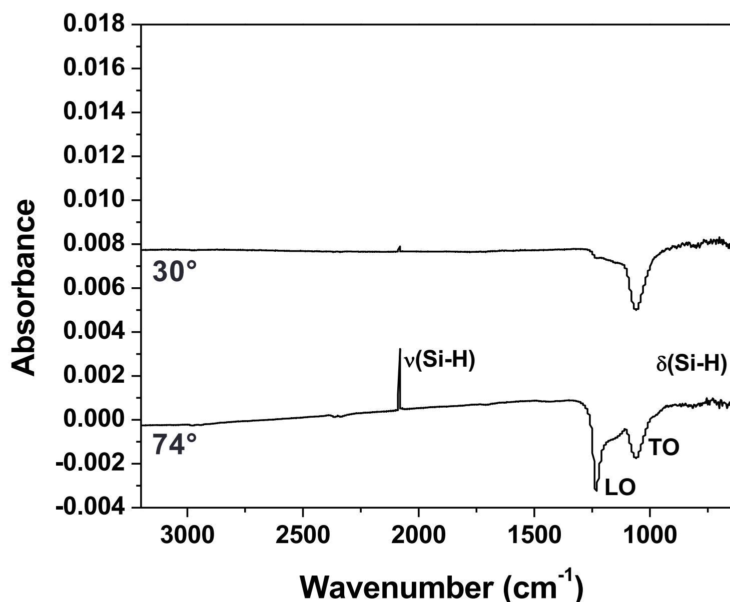

Figure 1.1. TIRS data for the H–Si(111) surface. The bottom spectrum was collected at 74° incidence angle and shows modes that are parallel or perpendicular to the surface. The top spectrum was collected at 30° incidence and primarily shows modes parallel to the surface. Si–H stretching (ν) and Si–H bending (δ) modes are indicated in the plot. The data is referenced to the SiO_x surface, and the negative peaks show the longitudinal optical (LO) and transverse optical (TO) Si–O–Si modes of the SiO_x surface.[15]

Si–H surfaces were shown to be capable of undergoing wet-chemical reaction with 1-alkenes and 1-alkynes via a hydrosilylation mechanism in 1995.[16] This discovery spurred a flurry of research aimed at achieving self-assembly of monolayers on Si–H surfaces and a new appreciation for the use of semiconductor surfaces as reactants in wet chemical reactions. Hydrosilylation of 1-alkenes and 1-alkynes on Si–H surfaces remains the most common, and one of the simplest, methods for imparting organic functionality to Si surfaces. Substrates prepared by hydrosilylation have been used to attach reversible redox species to the surface,[17-19] seed the growth of metal oxides by atomic layer deposition (ALD),[20-21] and attach biomolecules, such as DNA, to the surface.[22-23]

One of the major drawbacks of hydrosilylation reactions on Si–H surfaces is the mechanism by which it proceeds. The (111) crystal plane has the lowest density of reactive Si–H bonds and is, therefore, the least sterically crowded surface. Still, steric considerations preclude the smallest substrates suitable for undergoing hydrosilylation on H–Si(111) surfaces, such as acetylene or ethylene, from effectively terminating all of the reactive surface sites.[24] Incomplete termination of the Si surface with Si–C bonds leaves unreacted Si–H bonds on the surface, which are susceptible to the formation of surface electronic trap states, also known as surface states. Moreover, hydrosilylation has been proposed to occur via a radical mechanism that propagates across the surface, leaving a high density of surface states after the reaction completes.[25] The high density of surface states results in a high surface recombination velocity (*S*), which correlates with current lost to recombination at the interface and negatively impacts the energetics of surfaces prepared by hydrosilylation.

1.2 HALOGENATED SILICON SURFACES

Halogenated Si surfaces are typically used as intermediates in the synthesis of target semiconductor surfaces.[26-33] Chlorine-terminated Si (Si–Cl) surfaces, which are the most commonly used halogenated Si surface, have been prepared by methods that include the gas-phase reaction of Cl_2(g) with Si–H[34-40] or the solution phase reaction of PCl_5[28, 31, 33, 36, 41-43] with Si–H in chlorobenzene. The Si–Cl surface is the least sterically crowded of the halogenated surface, allowing for a greater density of Si–Cl bonds capable of undergoing reaction with an alkylating reagent. While all Si–Cl preparation methods yield Si–Cl bonds on the surface, different methods can yield different surface coverage and etch pit density. Bromine-terminated Si (Si–Br) surfaces can be prepared in similar ways by gas-phase reaction of Si–H surfaces with Br_2(g), solution phase reaction with Br_2(l), or solution phase reaction with *N*-bromosuccinamide.[44-47] Both Br and Cl are sterically able to terminate all Si atop sites on the (111) crystal plane, allowing for both Cl–Si(111) and Br–Si(111) surfaces to serve as generally interchangeable reactive surfaces in sample preparation.

Iodine terminated silicon (Si–I) surfaces have been prepared by reaction of Si–H surfaces with I_2 in benzene[48] and by exposure of vacuum-cleaned Si to CH_3I vapor.[49-51] The van der Waals radius of I is too large to terminate all Si(111) atop sites, and a maximum coverage of ~0.33 ML Si–I was observed for reaction of H–Si(111) with I_2/benzene. The steric bulk of I could be potentially exploited in order to form mixed monolayers on Si surfaces by partial iodination followed by reaction of the Si–I sites with Grignards and reaction of the residual Si–H sites by hydrosilylation. The differences in the reactivity of the Si–Cl, Si–Br, or Si–I surfaces have additionally not been clearly documented.

1.3 METHYL-TERMINATED SILICON SURFACES

Alkyl termination of Si surfaces by a two-step halogenation/alkylation procedure was first reported in 1996.[28] Generally, this two-step procedure involves the reaction of a Si–Cl or Si–Br intermediate surface with a Grignard, organolithium, or organosodium reagent.[15, 24, 26-27, 31-33, 52-53] This method allows for the facile and rapid attachment of short-chain alkyl groups, including methyl, ethyl, and phenyl, which would not be achievable by hydrosilylation chemistry. While long-chain alkyl groups are also readily attached by halogenation/alkylation, the interest in methyl-terminated Si(111) (CH_3–Si(111)) has been the most intense. The novelty of CH_3–Si(111) surfaces is centered around the unique ability of the –CH_3 group to terminate nearly all of the atop Si(111) sites,[54-58] affording CH_3–Si(111) surfaces exceptional chemical stability[26, 31-32] and very low surface recombination velocity.[59] While CH_3–Si(111) surfaces have been the subject of numerous scientific studies over two decades, my work as a graduate student initially focused on achieving control over the preparation of CH_3–Si(111) surfaces, and I reproduced much of the data that has been reported previously. The following section is a consolidated overview of CH_3–Si(111) surface characterization using the data I collected for control CH_3–Si(111) samples.

TIRS data for CH_3–Si(111) surfaces are given in Figure 1.2.[15] The C–H stretching (ν) region shows modes at 2961, 2926, 2910, and 2856 cm^{-1} with the signals at 2961 and 2910 cm^{-1} having been assigned to the asymmetric (ν_a) and symmetric (ν_s) C–H stretching motions of the –CH_3 group, respectively, and the signals at 2926 and 2856 cm^{-1} having been assigned to –CH_2– groups on adventitious C species. The presence of a signal at 1257

cm^{-1} at 74° with respect to the surface normal but not at 30° indicates the presence of a $(C–H)_{CH_3}$ symmetric bending (δ_s), or "umbrella," motion polarized perpendicular to the surface. This signal, in addition to a Si–C stretching peak at 678 cm^{-1} polarized perpendicular to the surface, provides a strong indication that the Si–CH_3 group is oriented normal to the surface. Additionally, a CH_3 rocking (ρ) mode at 753 cm^{-1} is observed at both angles of incidence.

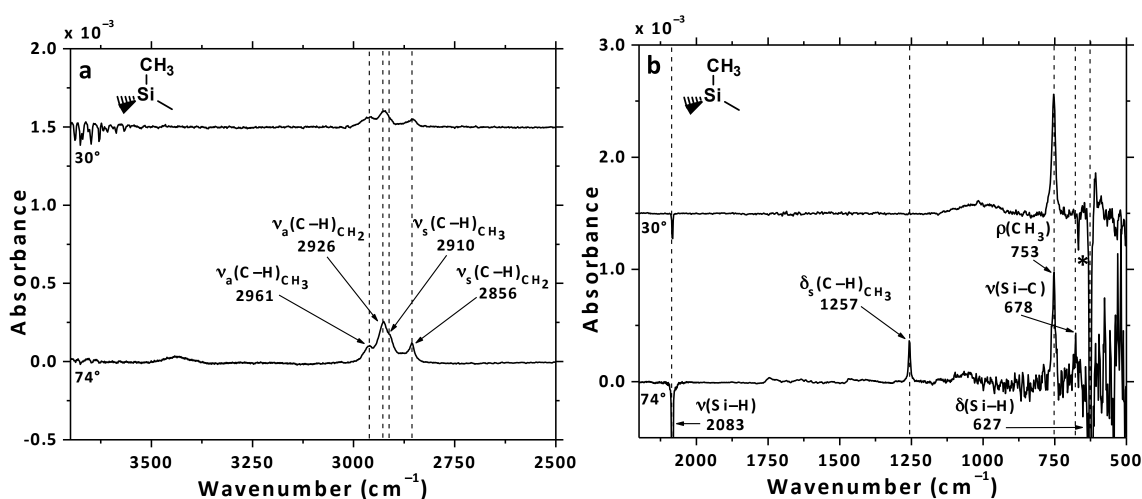

Figure 1.2. TIRS data for CH_3–Si(111) surfaces, referenced to the H–Si(111) surface, collected at 74° (bottom) and 30° (top) from the surface normal. Panel a shows high-energy region, and panel b shows the low-energy region. The negative peaks in panel b resulted from the H–Si(111) background. A sharp negative peak observed in panel b at 30° incidence marked with ∗ at 667 cm^{-1} resulted from CO_2 in the atmosphere. The subscripts "CH_3" and "CH_2" indicate C–H stretching signals arising from the –CH_3 and –CH_2– groups, respectively. The peak positions and assignments are indicated. The 30° spectrum is offset vertically for clarity.

HREELS data for CH_3–Si(111) surfaces,[60] shown in Figure 1.3, allows for detection of vibrational signals that could not be readily observed by TIRS. HREELS data for CH_3–Si(111) surfaces exhibited peaks centered at 747, 1267, and 2927 cm^{-1}, corresponding to CH_3 rocking, $(C–H)_{CH_3}$ symmetric bending, and $(C–H)_{CH_3}$ symmetric and asymmetric stretching motions, respectively, all of which were observed using TIRS. Resolution limitations of the HREELS instrumentation yielded a single C–H stretching peak for the asymmetric and symmetric stretching modes. The use of HREELS allowed for observation of Si–C stretching (665 cm^{-1}) and bending (477 cm^{-1}) signals in addition to the IR-inactive $(C–H)_{CH_3}$ asymmetric bending (δ_a) motion at 1399 a cm^{-1}. A small amount of silicon oxide (SiO_x) gave rise to a signal that was centered at 1066 cm^{-1}. These results compare favorably with previously published spectra of CH_3–Si(111) surfaces.

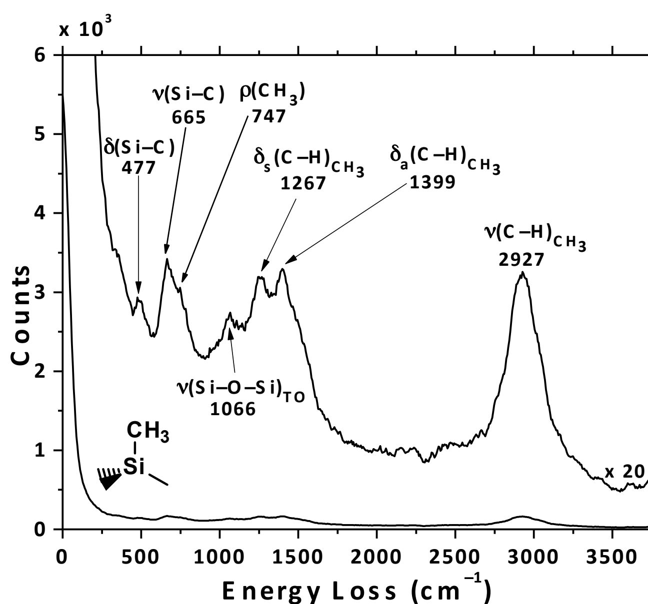

Figure 1.3. HREELS data for CH_3–Si(111) surfaces. The data were collected in the specular geometry using an incident beam energy of 5.0 eV, and the fwhm of the elastic peak was 13.3 meV. The raw spectrum (bottom) is shown with the magnified spectrum (top) superimposed for clarity. The peak positions and assignments are indicated in the figure.

Table 1.1 summarizes the vibrational modes detected by TIRS and HREELS for CH_3–Si(111) surfaces along with the orientation of the modes with respect to the surface plane.

Table 1.1. Summary of the Positions and Assigned Modes for the Vibrational Signatures Observed for the CH_3–Si(111) Surface.

TIRS Frequency (cm^{-1})	**HREELS Frequency (cm^{-1})[a]**	**Assigned Mode[b]**	**Orientation to Surface[c]**
2961	2927	$\nu_a(C–H)_{CH_3}$	
2926	2927	$\nu_a(C–H)_{CH_2}$	
2910	2927	$\nu_s(C–H)_{CH_3}$	
2856	2927	$\nu_s(C–H)_{CH_2}$	
–	1399	$\delta_a(C–H)_{CH_3}$	
1257	1267	$\delta_s(C–H)_{CH_3}$	$\perp$
weak	1066	$\nu(Si–O–Si)_{TO}$	not $\perp$
753	747	$\rho(CH_3)$	not $\perp$
678	665	ν(Si–C)	$\perp$
–	477	δ(Si–C)	

[a]In some cases, HREELS signals do not resolve multiple vibrational modes that are observed by TIRS. The HREELS signal with the closest energy to the resolved TIRS signal is paired in the table. [b]The symbols ν, δ, and ρ signify stretching, bending, and rocking motions, respectively, with subscripts a and s indicating whether the mode is asymmetric or symmetric, respectively. Subscripts "CH_3" and "CH_2" indicate C–H stretching signals arising from $–CH_3$ and $–CH_2–$ saturated hydrocarbons, respectively. The subscript "TO" indicates a transverse optical Si–O–Si motion. [c]The orientation of the vibrational mode with respect to the plane of the sample surface determined by TIRS is given.

X-ray photoelectron spectroscopy (XPS) data provides quantitative information about the species present on CH_3–Si(111) surfaces. Survey spectra indicate that only signals ascribable to Si, C, and O are observed, and high-resolution spectra are shown for the C 1s and Si 2p core levels in Figure 1.4. CH_3–Si(111) surfaces exhibit three distinct C 1s signals, the most prominent of which is centered at 284.3 eV. This photoemission peak is ascribed to C bonded to Si (C_{Si}),[61] while the remaining two signals at 285.2 and 286.4 eV arise from adventitious C species. The fractional monolayer coverage (Φ) of $-CH_3$ groups on the prepared CH_3–Si(111) surfaces can be estimated using a substrate-overlayer model discussed in Chapter 2 (section 2.2.3),[62-63] to yield Φ_{Si-CH_3} =1.13 ± 0.07 ML, which supports the conclusion that CH_3–Si(111) surfaces exhibit nearly full termination of the Si atop sites with Si–C bonds. While the calculated Φ_{Si-CH_3} is higher than the maximum 1 ML of $-CH_3$ groups, the reported value is fairly typical for the magnitude of error expected when quantifying XPS data. Only the photoemission signal at 284.3 eV was used in the estimation of Φ_{Si-CH_3} because this signal arises directly from the bound $-CH_3$ group. Previous work has shown that annealing CH_3–Si(111) surfaces to 450 °C in vacuum removes the majority of adventitious species and reveals two additional C 1s photoemission signals resulting from the vibrational fine structure of the $-CH_3$ group.[61, 64] However, due to resolution limitations of the instrumentation used in this work, these peaks are omitted from the fitting process for all alkyl-terminated surfaces. No detectable amount of SiO_x was observed by XPS on CH_3–Si(111) surfaces.

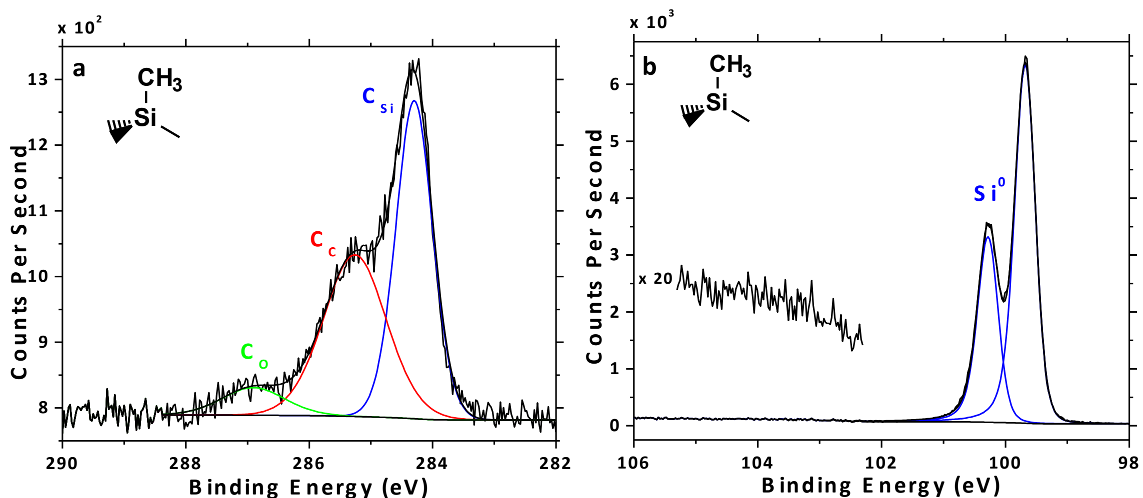

Figure 1.4. High-resolution XP spectra of the (a) C 1s and (b) Si 2p regions for CH_3–Si(111) surfaces. The low binding-energy C photoemission signal at 284.3 eV has been ascribed to C bound to Si (blue, C_{Si}), with the C 1s signals at 285.2 and 286.4 eV arising from C bound to C (red, C_C) and C bound to O (green, C_O), respectively. The region from 102–105 eV in the Si 2p spectrum is magnified to show the absence of detectable high-order SiO_x.

Figure 1.5 gives a representative atomic-force microscope (AFM) image of a CH_3–Si(111) surface. The surface generally exhibits broad atomic terraces with relatively few etch pits. The difference in height observed at terrace step edges is ~0.3 nm, which is consistent with the height difference between terraces observed on vacuum cleaved unreconstructed Si(111) surfaces.[65] The surfaces often exhibit particulates that are shown as raised spots in the AFM images. The size and concentration of these spots tends to vary, and could be correlated with the batch and manufacturer of the Grignard reagent (CH_3MgCl) used in the synthesis process. XPS data shows no detectable metal contaminants, suggesting that these spots are organic in nature and could be the physical manifestation of the adventitious carbon observed in high-resolution C 1s XP spectra of CH_3–Si(111) surfaces.

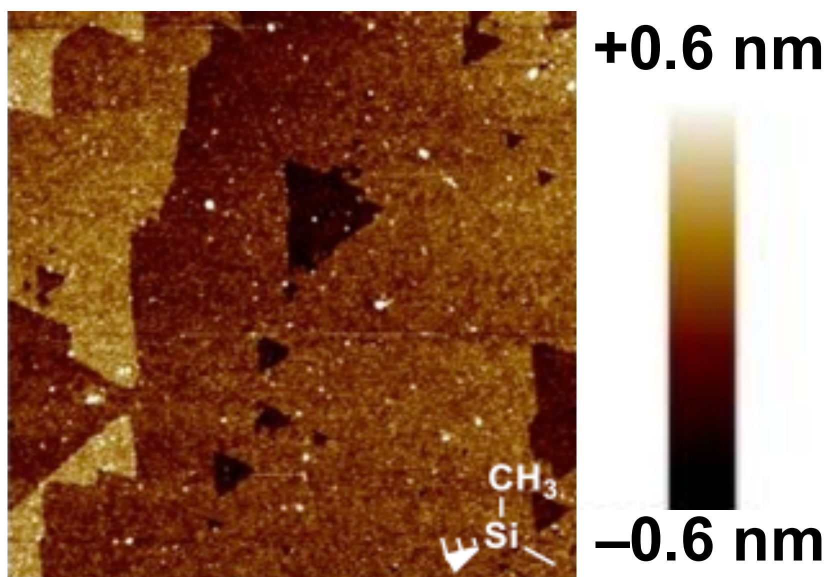

Figure 1.5. Representative topographical AFM image of the CH_3–Si(111) surface. The image is 1 µm × 1 µm with a z-scale of 1.2 nm (–0.6 to +0.6 nm).

Figure 1.6 shows a representative low-energy electron diffraction (LEED) image collected for a CH_3–Si(111) surface.[61] The LEED pattern exhibits 3-fold symmetry, which is indicative of a (1 × 1) surface unit cell. The image pictured shows 6 bright spots of approximately equal intensity. Adjusting the energy slightly above or below the 43 eV incident beam energy in Figure 1.6 reveals the 3-fold symmetry, as 3 spots remain bright and 3 spots lower in intensity. The spots appear as very bright and sharp relative to the background. This high contrast between the diffraction spots and the background is a strong indication that the CH_3–Si(111) surface exhibits exceptional long-range ordering. Thus, the LEED data supports the conclusion that CH_3–Si(111) surfaces are exceptionally well-ordered and have nearly complete termination of the atop Si sites with Si–C bonds.

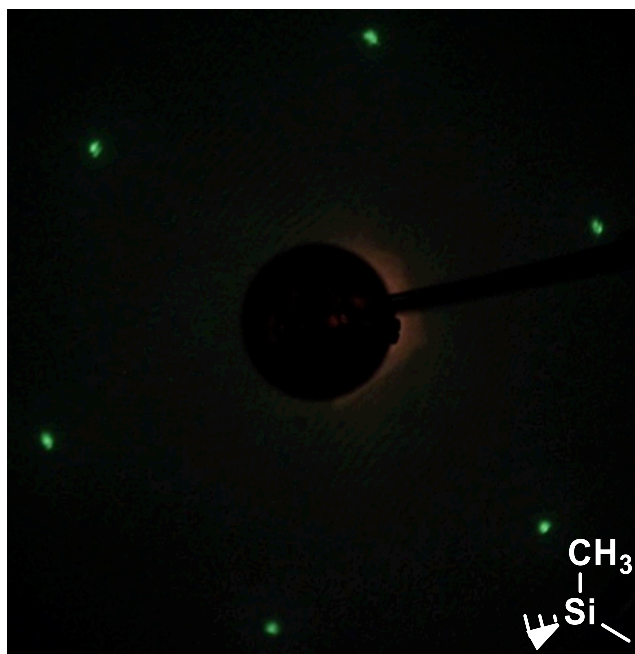

Figure 1.6. Representative LEED pattern for a CH_3–Si(111) surface collected at 43 eV incident beam energy.

Surface recombination velocity (*S*) measurements are typically acquired using a time-resolved microwave conductivity setup, but can also be measured using time-resolved radio frequency conductivity measurements. The microwave conductivity setup used in this work is described in detail in section 2.2.2. The microwave conductivity decay curves can be fitted to an exponential decay to obtain a charge carrier recombination lifetime, τ. Section 2.2.3 describes how to convert τ to a surface recombination velocity in cm s^{-1}. A decrease in *S* represents a decrease in the electrically active surface state density. Figure 1.7 shows *S* for a CH_3–Si(111) surface as a function of exposure to air. A typical initial *S* for a CH3–Si(111) surface immediately after preparation and cleaning was 40 cm s^{-1}, which corresponds to an electrical defect density of 1 defect per 2×10^5 surface sites (eq 2.4).[66] Remarkably, *S* for CH_3–Si(111) surfaces decreases to ~15 cm s^{-1} after 72 h exposure to air. This decrease results in a lower surface state density of 1 per 5×10^5 surface sites. Over

time, a small increase in S is typically observed, but the increase does not represent a significant increase in the electrically active surface state density. Over the same amount of time, the CH_3–Si(111) surface would be expected to form a measureable amount of SiO_x,[31] but the formation of SiO_x does not appear to contribute significantly to an increase in S. One hypothesis for the initial decrease in S observed over the first 72 h of air exposure could involve the initial passivation of surface states, such as dangling bonds, by reaction with H_2O and O_2 in the air, with long-term oxidation of the surface in air having little effect on S. This is in contrast to H–Si(111) surfaces, which undergo comparatively rapid oxidation in air, and exhibit high S after just 15 min air exposure.[59] Thus, CH_3–Si(111) surfaces exhibit improved stability in air relative to H–Si(111) surfaces and have remarkable electrical properties.

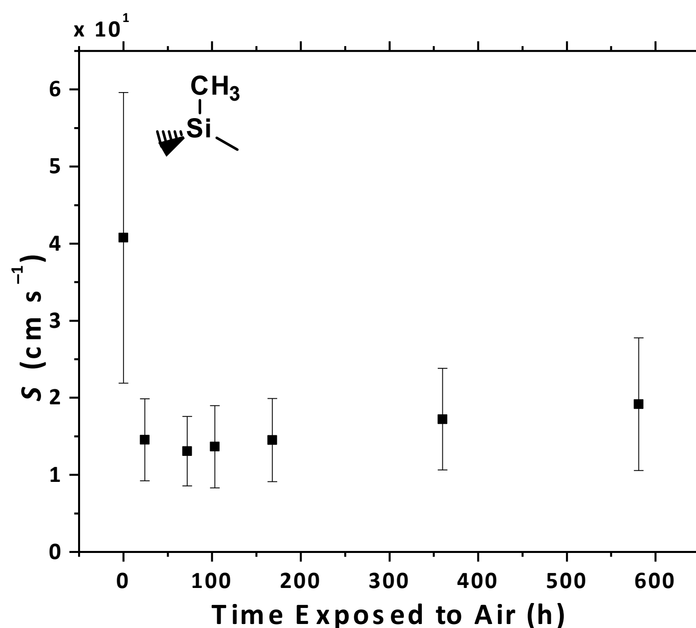

Figure 1.7. S behavior as a function of time exposed to air for CH_3–Si(111) surfaces. The error bars represent 1 standard deviation about the mean.

1.4 SURFACE CHEMISTRY APPLICATIONS

Functionalization of semiconductor surfaces is motivated by a variety of applications, often inspired by the conventional uses for semiconductors in transistors, photovoltaics, and photoelectrochemical cells. In particular, surface chemistry offers the opportunity to control the interface between semiconductors and other functional device components, which may include catalysts, metals, conductive polymers, or protecting layers (e.g. metal oxides). Organic scaffolds grafted to semiconductor surfaces can potentially allow for molecular-level control over the interface between the semiconductor and other device components to achieve optimal interactions from a mechanical, physical, and electrical perspective.

As part of the development of efficient and cost-effective photoelectrochemical water splitting cells for fuel generation, the interface between catalysts and semiconductors, depicted in Figure 1.8, is critical to the performance of the device. The catalyst/semiconductor must exhibit favorable mechanical interactions such that the catalyst remains closely associated with the surface, but the energetics at the interface must be favorable to effect the maximum output potential. Surface chemistry provides an exceptional opportunity to control the mechanical properties of the catalyst/semiconductor interface while also allowing for favorable energetics at the interface.

Some of the common catalysts that have been developed for use in photoelectrochemical water splitting cells include Pt, $MoSe_2$,[67] CoP,[68] and Fe_3P[69] for proton reduction and IrO_2 and NiO_x[70-71] for water oxidation. These catalysts are all metals, metal oxides, or alloys that have defined work functions that may not form highly rectifying junctions between Si and the catalyst. Additionally, these catalysts can be

deposited by a number of methods, including electrodeposition, drop-cast and sinter, or oxidation of a metallic film. Surface chemistry can be used to (1) tune the semiconductor band edges such that the energetics at the semiconductor/catalyst interface produces the maximum output voltage and (2) to improve the mechanical and physical robustness of the semiconductor/catalyst interaction so the catalyst film or particles remain bound to the semiconductor during long-term device operation. Organic linkers between Si and the catalysts could provide a scalable and robust method of improving Si/catalyst interfaces to achieve the properties required my photoelectrochemical systems.

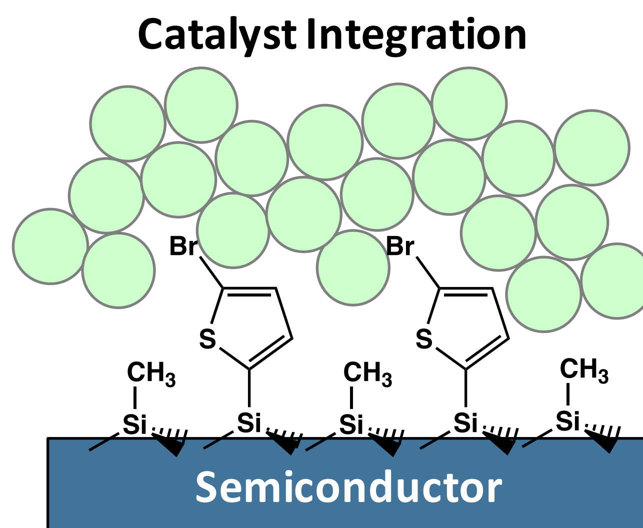

Figure 1.8. Example of linker chemistry that could be used to integrate catalyst nanoparticles (green circles) with semiconductor surfaces. The linker would be designed to impart a favorable surface dipole that positions the semiconductor band edges relative to the catalyst work function to effect the maximum device performance. Additionally, the mechanical interaction between the Si and the catalyst would be improved by the organic linker layer.

Related to Si/catalyst interfaces are Si/metal interfaces (Figure 1.9). The photovoltaic and transistor industries commonly form silicon/metal interfaces in

established device manufacturing processes. In some cases, an ohmic Si/metal contact is desired, while other applications require a rectifying Si/metal interaction. Deposition of metals directly on Si–H surfaces by common materials processing methods (e.g. evaporation and sputtering) typically results in the formation of metal silicides that are detrimental to the formation of rectifying contacts. Even soft deposition methods, such as electrodeposition or drop-cast and sinter, can yield high surface recombination velocity because of the propensity of the Si–H surface to oxidize and form surface states.

Organic modification of Si surfaces with molecules that impart a surface dipole that favorably positions the semiconductor band edges to effect the maximum energy out of the

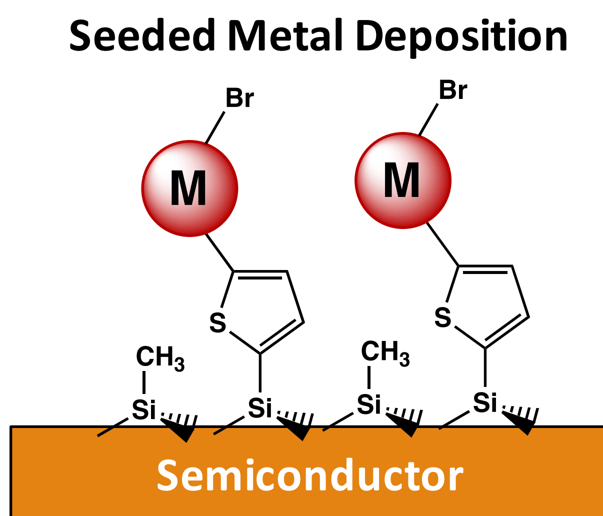

Figure 1.9. Example of linker chemistry that could be used to control metal deposition on a Si surface. The surface chemistry can be used to impart favorable band-edge positions to produce a maximum voltage at the Si/metal interface. Additionally, the reactivity of organic groups on the surface can be exploited to direct metal deposition and form nanopatterns on the surface.

Si/metal interface. Organic modification, such as methyl termination, has been demonstrated to allow for metals that typically form metal silicides, such as Au, to be

deposited on CH_3–Si(111) surfaces by soft deposition methods (e.g. electrodeposition or drop-cast and sinter).[72-73] Additionally, many organic groups, such as the C–Br bond in Figure 1.9, are reactive towards metals in solution and could be used to direct and control the deposition of metals on semiconductor surfaces. By pattering the surface with reactive organic groups, metals can conceivably be deposited in a controlled manner to yield nanopatterned semiconductor/metal contacts. Organic modification of silicon surfaces offers a unique opportunity to achieve unprecedented control over the deposition of metals on semiconductor surfaces.

Hybrid organic/inorganic solar cells have been developed as alternatives to conventional photovoltaics and photoelectrochemical cells. The polymer can serve as a light absorber as well as a conductive medium to direct charge transfer in solid state devices. Additionally, conductive polymers are generally less susceptible to oxidation or corrosion than inorganic semiconductors and thus could potentially be used as protection layers in photoelectrochemical cells. Moreover, polymer layers are typically flexible, and the development of robust semiconductor/polymer interfaces could allow for the development of improved flexible devices that are more cost effective than traditional photovoltaics.

Covalent bonding between silicon and monomer units for polymers, including thiophene and other conductive polymers,[45, 74-75] has been investigated previously. Figure 1.10 gives an example in which the monomer 3,4-ethylenedioxythiophene is used to covalently bind poly(3,4,-ethylenedioxythiophene) to the Si surface. The electrical properties of the silicon/polymer junction could conceivably be influenced by the nature of

the bonding at the Si/polymer interface, with covalent bonds allowing for improved interfacial conductivity and performance. In particular, poly(3,4,-ethylenedioxythiophene) (PEDOT)-poly(styrenesulfonate) (PSS) has been proposed for use in photoelectrochemical devices as a means of providing an ohmic electrical contact between the photoanode and photocathode, while allowing for proton transfer through the membrane and flexibility of the device.[76] Silicon surface chemistry offers a means of providing molecular-level control over the interface between silicon and conductive polymers in order to develop efficient and novel device architectures.

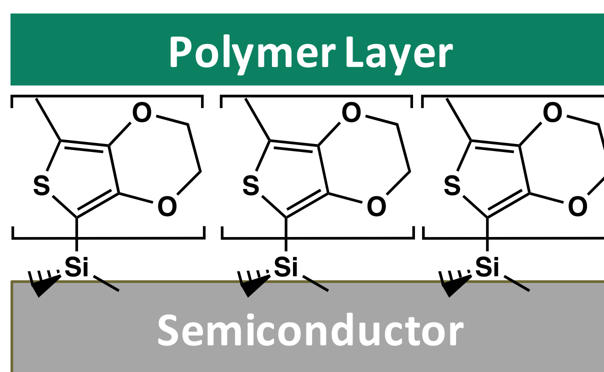

Figure 1.10. Example of a silicon/polymer junction formed by a covalent bond between the two materials. The surface of Si could be modified with monomers, in this case 3,4-ethylenedioxythiophene, and electropolymerization of the corresponding conductive polymer on the surface could allow for improved electrical conductivity and performance.

One of the current most challenging aspects in the development of stable and cost effective photoelectrochemical cells for water splitting is the corrosion or passivation of photoanodes in aqueous electrolyte. Silicon, for example, rapidly oxidizes and passivates, forming an electrically insulating layer on the surface, when used as a photoanode without

sufficient protection from oxidation on the surface. Recently, metal oxide layers, such as TiO_2 and NiO_x, deposited on Si substrates by atomic-layer deposition (ALD) or sputtering have been shown to allow for long-term operation of Si and other semiconductors as photoanodes.[70-71, 77] The interface between the Si and the metal oxide could conceivably be controlled on a molecular level by seeding the metal oxide deposition on the surface using a molecular scaffold that is reactive toward the metal oxide precursor.

Currently, semiconductors are most widely used by the microelectronics industry, which has increasingly relied on semiconductor-based integrated circuit technology to manufacture increasingly powerful computers and other electronic devices. A common motif in integrated circuit technology is the development of increasingly smaller nodes in the pursuit of increased power efficiency and performance. Currently, 14 nm nodes are the smallest commercially available technology, with 10 nm nodes set to be available in the near future. At such small node sizes, the surface of the semiconductor material becomes a significantly larger percentage of the overall node. The deposition of metal oxides, which are commonly used as gate materials in processor nodes, by ALD can be controlled using surface chemistry to direct the metal oxide deposition. Figure 1.11 presents an example of using reactive surface groups, such as aldehydes or alcohols, to direct the assembly of ALD-grown films, like aluminum oxide or titanium dioxide, on silicon surfaces.

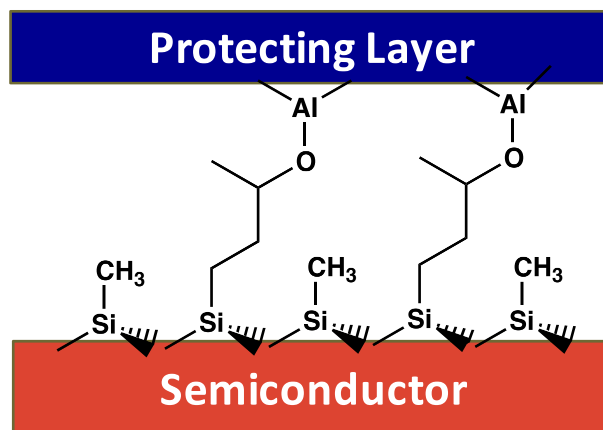

Figure 1.11. Example of a silicon/metal oxide junction formed by atomic layer deposition of trimethylaluminum (TMA) on a mixed methyl/propionaldehyde surface. The aldehyde groups on the surface are reactive toward the TMA precursor, allowing for growth of the TMA to be controlled by the chemical nature of the surface.[21]

This thesis presents a collection of studies that are intended to advance the field of silicon surface chemistry toward achieving the applications described above. Chapters 2 and 3 are focused on the characterization of short-chain unsaturated alkyl groups covalently bound to Si and investigating the reactivity of these groups. This work is broadly applicable to the development of improved interfacial chemistries at Si interfaces. Chapter 4 is focused on achieving control over the molecular surface dipole and band-edge positions through surface functionalization in order to improve the interfaces between silicon and the functional device components described above. Finally, Chapter 5 describes a mechanistic study into the reaction of H–Si(111) surfaces with methanol to improve the understanding of self-limiting, molecular charge transfer reactions at Si surfaces.

1.5 REFERENCES

1. Buriak, J. M. Organometallic Chemistry on Silicon and Germanium Surfaces. *Chem. Rev.* **2002**, *102*, 1271-1308.
2. Wayner, D. D. M.; Wolkow, R. A. Organic Modification of Hydrogen Terminated Silicon Surfaces. *Journal of the Chemical Society, Perkin Transactions 2* **2002**, 23-34.
3. Bent, S. F. Organic Functionalization of Group IV Semiconductor Surfaces: Principles, Examples, Applications, and Prospects. *Surf. Sci.* **2002**, *500*, 879-903.
4. Neergaard Waltenburg, H.; Yates, J. T. Surface Chemistry of Silicon. *Chem. Rev.* **1995**, *95*, 1589-1673.
5. Ibach, H.; Rowe, J. E. Hydrogen Adsorption and Surface Structures of Silicon. *Surf. Sci.* **1974**, *43*, 481-492.
6. Rappich, J.; Lewerenz, H. J. In Situ Fourier Transform Infrared Investigation on the Electrolytic Hydrogenation of n-Silicon (111). *J. Electrochem. Soc.* **1995**, *142*, 1233-1237.
7. Dittrich, T.; Rauscher, S.; Bitzer, T.; Aggour, M.; Flietner, H.; Lewerenz, H. J. Electronic Properties of n-Si(111) during Electrochemical Surface Transformation toward H-Termination. *J. Electrochem. Soc.* **1995**, *142*, 2411-2413.
8. Rappich, J.; Jungblut, H.; Aggour, M.; Lewerenz, H. J. Electrochemical Smoothing of Silicon (111). *J. Electrochem. Soc.* **1994**, *141*, L99-L102.
9. Bitzer, T.; Gruyters, M.; Lewerenz, H. J.; Jacobi, K. Electrochemically Prepared Si(111) 1×1-H Surface. *Appl. Phys. Lett.* **1993**, *63*, 397-399.

10. Burrows, V. A.; Chabal, Y. J.; Higashi, G. S.; Raghavachari, K.; Christman, S. B. Infrared Spectroscopy of Si(111) Surfaces after HF Treatment: Hydrogen Termination and Surface Morphology. *Appl. Phys. Lett.* **1988**, *53*, 998-1000.

11. Chabal, Y. J.; Higashi, G. S.; Raghavachari, K.; Burrows, V. A. Infrared Spectroscopy of Si(111) and Si(100) Surfaces after HF Treatment: Hydrogen Termination and Surface Morphology. *J. Vac. Sci. Technol. A* **1989**, *7*, 2104-2109.

12.Clark, I. T.; Aldinger, B. S.; Gupta, A.; Hines, M. A. Aqueous Etching Produces Si(100) Surfaces of Near-Atomic Flatness: Strain Minimization Does Not Predict Surface Morphology. *J. Phys. Chem. C* **2010**, *114*, 423-428.

13. Weinberger, B. R.; Peterson, G. G.; Eschrich, T. C.; Krasinski, H. A. Surface Chemistry of HF Passivated Silicon: X-ray Photoelectron and Ion Scattering Spectroscopy Results. *J. Appl. Phys.* **1986**, *60*, 3232-3234.

14. Higashi, G. S.; Chabal, Y. J.; Trucks, G. W.; Raghavachari, K. Ideal Hydrogen Termination of the Si (111) Surface. *Appl. Phys. Lett.* **1990**, *56*, 656-658.

15. Webb, L. J.; Rivillon, S.; Michalak, D. J.; Chabal, Y. J.; Lewis, N. S. Transmission Infrared Spectroscopy of Methyl- and Ethyl-Terminated Silicon(111) Surfaces. *J. Phys. Chem. B* **2006**, *110*, 7349-7356.

16. Linford, M. R.; Fenter, P.; Eisenberger, P. M.; Chidsey, C. E. D. Alkyl Monolayers on Silicon Prepared from 1-Alkenes and Hydrogen-Terminated Silicon. *J. Am. Chem. Soc.* **1995**, *117*, 3145-3155.

17. Lattimer, J. R. C.; Blakemore, J. D.; Sattler, W.; Gul, S.; Chatterjee, R.; Yachandra, V. K.; Yano, J.; Brunschwig, B. S.; Lewis, N. S.; Gray, H. B. Assembly, Characterization,

and Electrochemical Properties of Immobilized Metal Bipyridyl Complexes on Silicon(111) Surfaces. *Dalton Trans.* **2014**, *43*, 15004-15012.

18. Lattimer, J. R. C.; Brunschwig, B. S.; Lewis, N. S.; Gray, H. B. Redox Properties of Mixed Methyl/Vinylferrocenyl Monolayers on Si(111) Surfaces. *J. Phys. Chem. C* **2013**, *117*, 27012-27022.
19. O'Leary, L. E.; Rose, M. J.; Ding, T. X.; Johansson, E.; Brunschwig, B. S.; Lewis, N. S. Heck Coupling of Olefins to Mixed Methyl/Thienyl Monolayers on Si(111) Surfaces. *J. Am. Chem. Soc.* **2013**, *135*, 10081-10090.
20. Li, M.; Dai, M.; Chabal, Y. J. Atomic Layer Deposition of Aluminum Oxide on Carboxylic Acid-Terminated Self-Assembled Monolayers. *Langmuir* **2009**, *25*, 1911-1914.
21. O'Leary, L. E.; Strandwitz, N. C.; Roske, C. W.; Pyo, S.; Brunschwig, B. S.; Lewis, N. S. Use of Mixed CH_3–/$HC(O)CH_2CH_2$–Si(111) Functionality to Control Interfacial Chemical and Electronic Properties During the Atomic-Layer Deposition of Ultrathin Oxides on Si(111). *J. Phys. Chem. Lett.* **2015**, *6*, 722-726.
22. Strother, T.; Cai, W.; Zhao, X.; Hamers, R. J.; Smith, L. M. Synthesis and Characterization of DNA-Modified Silicon (111) Surfaces. *J. Am. Chem. Soc.* **2000**, *122*, 1205-1209.
23. Strother, T.; Hamers, R. J.; Smith, L. M. Covalent Attachment of Oligodeoxyribonucleotides to Amine-Modified Si (001) Surfaces. *Nucleic Acids Res.* **2000**, *28*, 3535-3541.

24. Nemanick, E. J.; Solares, S. D.; Goddard, W. A.; Lewis, N. S. Quantum Mechanics Calculations of the Thermodynamically Controlled Coverage and Structure of Alkyl Monolayers on Si(111) Surfaces. *J. Phys. Chem. B* **2006**, *110*, 14842-14848.

25. Lehner, A.; Kohl, F.; Franzke, S. A.; Graf, T.; Brandt, M. S.; Stutzmann, M. Photoconductivity and Spin-Dependent Photoconductivity of Hydrosilylated (111) Silicon Surfaces. *Appl. Phys. Lett.* **2003**, *82*, 565-567.

26. Bansal, A.; Lewis, N. S. Stabilization of Si Photoanodes in Aqueous Electrolytes through Surface Alkylation. *J. Phys. Chem. B* **1998**, *102*, 4058-4060.

27. Bansal, A.; Lewis, N. S. Electrochemical Properties of (111)-Oriented n-Si Surfaces Derivatized with Covalently-Attached Alkyl Chains. *J. Phys. Chem. B* **1998**, *102*, 1067-1070.

28. Bansal, A.; Li, X.; Lauermann, I.; Lewis, N. S.; Yi, S. I.; Weinberg, W. H. Alkylation of Si Surfaces Using a Two-Step Halogenation/Grignard Route. *J. Am. Chem. Soc.* **1996**, *118*, 7225-7226.

29. Tian, F.; Taber, D. F.; Teplyakov, A. V. –NH– Termination of the Si(111) Surface by Wet Chemistry. *J. Am. Chem. Soc.* **2011**, *133*, 20769-20777.

30. Tian, F.; Teplyakov, A. V. Silicon Surface Functionalization Targeting Si–N Linkages. *Langmuir* **2013**, *29*, 13-28.

31. Webb, L. J.; Lewis, N. S. Comparison of the Electrical Properties and Chemical Stability of Crystalline Silicon(111) Surfaces Alkylated Using Grignard Reagents or Olefins with Lewis Acid Catalysts. *J. Phys. Chem. B* **2003**, *107*, 5404-5412.

32. Webb, L. J.; Michalak, D. J.; Biteen, J. S.; Brunschwig, B. S.; Chan, A. S. Y.; Knapp, D. W.; Meyer, H. M.; Nemanick, E. J.; Traub, M. C.; Lewis, N. S. High-Resolution

Soft X-ray Photoelectron Spectroscopic Studies and Scanning Auger Microscopy Studies of the Air Oxidation of Alkylated Silicon(111) Surfaces. *J. Phys. Chem. B* **2006**, *110*, 23450-23459.

33. Webb, L. J.; Nemanick, E. J.; Biteen, J. S.; Knapp, D. W.; Michalak, D. J.; Traub, M. C.; Chan, A. S. Y.; Brunschwig, B. S.; Lewis, N. S. High-Resolution X-ray Photoelectron Spectroscopic Studies of Alkylated Silicon(111) Surfaces. *J. Phys. Chem. B* **2005**, *109*, 3930-3937.
34. Zhu, X. Y.; Boiadjiev, V.; Mulder, J. A.; Hsung, R. P.; Major, R. C. Molecular Assemblies on Silicon Surfaces via Si−O Linkages. *Langmuir* **2000**, *16*, 6766-6772.
35. Terry, J.; Mo, R.; Wigren, C.; Cao, R.; Mount, G.; Pianetta, P.; Linford, M. R.; Chidsey, C. E. D. Reactivity of the H–Si(111) Surface. *Nuclear Instruments and Methods in Physics Research Section B: Beam Interactions with Materials and Atoms* **1997**, *133*, 94-101.
36. Rivillon, S.; Chabal, Y. J.; Webb, L. J.; Michalak, D. J.; Lewis, N. S.; Halls, M. D.; Raghavachari, K. Chlorination of Hydrogen-Terminated Silicon (111) Surfaces. *J. Vac. Sci. Technol. A* **2005**, *23*, 1100-1106.
37. Florio, J. V.; Robertson, W. D. Chlorine Reactions on the Si(111) Surface. *Surf. Sci.* **1969**, *18*, 398-427.
38. Li, Z.; Kamins, T. I.; Li, X.; Williams, R. S. Chlorination of Si Surfaces with Gaseous Hydrogen Chloride at Elevated Temperatures. *Surf. Sci.* **2004**, *554*, L81-L86.
39. Rivillon, S.; Amy, F.; Chabal, Y. J.; Frank, M. M. Gas Phase Chlorination of Hydrogen-Passivated Silicon Surfaces. *Appl. Phys. Lett.* **2004**, *85*, 2583-2585.

40. Eves, B. J.; Lopinski, G. P. Formation and Reactivity of High Quality Halogen Terminated Si(111) Surfaces. *Surf. Sci.* **2005**, *579*, 89-96.

41. Bansal, A.; Li, X.; Yi, S. I.; Weinberg, W. H.; Lewis, N. S. Spectroscopic Studies of the Modification of Crystalline Si(111) Surfaces with Covalently-Attached Alkyl Chains Using a Chlorination/Alkylation Method. *J. Phys. Chem. B* **2001**, *105*, 10266-10277.

42. Cao, P.; Xu, K.; Heath, J. R. Azidation of Silicon(111) Surfaces. *J. Am. Chem. Soc.* **2008**, *130*, 14910-14911.

43. Yu, H.; Webb, L. J.; Heath, J. R.; Lewis, N. S. Scanning Tunneling Spectroscopy of Methyl- and Ethyl-Terminated Si(111) Surfaces. *Appl. Phys. Lett.* **2006**, *88*, -.

44. Gleason-Rohrer, D. C.; Brunschwig, B. S.; Lewis, N. S. Measurement of the Band Bending and Surface Dipole at Chemically Functionalized Si(111)/Vacuum Interfaces. *J. Phys. Chem. C* **2013**, *117*, 18031-18042.

45. He, J.; Patitsas, S. N.; Preston, K. F.; Wolkow, R. A.; Wayner, D. D. M. Covalent Bonding of Thiophenes to Si(111) by a Halogenation/Thienylation Route. *Chem. Phys. Lett.* **1998**, *286*, 508-514.

46. Li, Y.; O'Leary, L. E.; Lewis, N. S.; Galli, G. Combined Theoretical and Experimental Study of Band-Edge Control of Si through Surface Functionalization. *J. Phys. Chem. C* **2013**, *117*, 5188-5194.

47. Plymale, N. T.; Kim, Y.-G.; Soriaga, M. P.; Brunschwig, B. S.; Lewis, N. S. Synthesis, Characterization, and Reactivity of Ethynyl- and Propynyl-Terminated Si(111) Surfaces. *J. Phys. Chem. C* **2015**, *119*, 19847-19862.

48. Cai, W.; Lin, Z.; Strother, T.; Smith, L. M.; Hamers, R. J. Chemical Modification and Patterning of Iodine-Terminated Silicon Surfaces Using Visible Light. *J. Phys. Chem. B* **2002**, *106*, 2656-2664.

49. Gutleben, H.; Lucas, S. R.; Cheng, C. C.; Choyke, W. J.; Yates, J. T. Thermal Stability of the Methyl Group Adsorbed on Si(100): CH_3I Surface Chemistry. *Surf. Sci.* **1991**, *257*, 146-156.

50. Colaianni, M. L.; Chen, P. J.; Gutleben, H.; Yates, J. T. Vibrational Studies of CH_3I on Si(100)-(2×1): Adsorption and Decomposition of the Methyl Species. *Chem. Phys. Lett.* **1992**, *191*, 561-568.

51. Kong, M. J.; Lee, S. S.; Lyubovitsky, J.; Bent, S. F. Infrared Spectroscopy of Methyl Groups on Silicon. *Chem. Phys. Lett.* **1996**, *263*, 1-7.

52. Nemanick, E. J.; Hurley, P. T.; Brunschwig, B. S.; Lewis, N. S. Chemical and Electrical Passivation of Silicon (111) Surfaces through Functionalization with Sterically Hindered Alkyl Groups. *J. Phys. Chem. B* **2006**, *110*, 14800-14808.

53. Nemanick, E. J.; Hurley, P. T.; Webb, L. J.; Knapp, D. W.; Michalak, D. J.; Brunschwig, B. S.; Lewis, N. S. Chemical and Electrical Passivation of Single-Crystal Silicon(100) Surfaces through a Two-Step Chlorination/Alkylation Process. *J. Phys. Chem. B* **2006**, *110*, 14770-14778.

54. Becker, J. S.; Brown, R. D.; Johansson, E.; Lewis, N. S.; Sibener, S. J. Helium Atom Diffraction Measurements of the Surface Structure and Vibrational Dynamics of CH_3--Si(111) and CD_3--Si(111) Surfaces. *J. Chem. Phys.* **2010**, *133*, 104705.

55. Brown, R. D.; Hund, Z. M.; Campi, D.; O'Leary, L. E.; Lewis, N. S.; Bernasconi, M.; Benedek, G.; Sibener, S. J. Hybridization of Surface Waves with Organic Adlayer

Librations: A Helium Atom Scattering and Density Functional Perturbation Theory Study of Methyl-Si(111). *Phys. Rev. Lett.* **2013**, *110*, 156102.

56. Brown, R. D.; Hund, Z. M.; Campi, D.; O'Leary, L. E.; Lewis, N. S.; Bernasconi, M.; Benedek, G.; Sibener, S. J. The Interaction of Organic Adsorbate Vibrations with Substrate Lattice Waves in Methyl-Si(111)-(1 × 1). *J. Chem. Phys.* **2014**, *141*, 024702.
57. Nihill, K. J.; Hund, Z. M.; Muzas, A.; Díaz, C.; del Cueto, M.; Frankcombe, T.; Plymale, N. T.; Lewis, N. S.; Martín, F.; Sibener, S. J. Experimental and Theoretical Study of Rotationally Inelastic Diffraction of $H_2(D_2)$ from Methyl-Terminated Si(111). *J. Chem. Phys.* **2016**, *145*, 084705.
58. Yu, H.; Webb, L. J.; Ries, R. S.; Solares, S. D.; Goddard, W. A.; Heath, J. R.; Lewis, N. S. Low-Temperature STM Images of Methyl-Terminated Si(111) Surfaces. *J. Phys. Chem. B* **2004**, *109*, 671-674.
59. Royea, W. J.; Juang, A.; Lewis, N. S. Preparation of Air-Stable, Low Recombination Velocity Si(111) Surfaces through Alkyl Termination. *Appl. Phys. Lett.* **2000**, *77*, 1988-1990.
60. Yamada, T.; Kawai, M.; Wawro, A.; Suto, S.; Kasuya, A. HREELS, STM, and STS study of CH_3-Terminated Si(111)-(1 x 1) Surface. *J. Chem. Phys.* **2004**, *121*, 10660-10667.
61. Hunger, R.; Fritsche, R.; Jaeckel, B.; Jaegermann, W.; Webb, L. J.; Lewis, N. S. Chemical and Electronic Characterization of Methyl-Terminated Si(111) Surfaces by High-Resolution Synchrotron Photoelectron Spectroscopy. *Phys. Rev. B* **2005**, *72*, 045317.

62. Briggs, D.; Seah, M. P. *Practical Surface Analysis: Auger and X-ray Photoelectron Spectroscopy*, 2nd ed.; John Wiley & Sons, Inc.: New York, 1990; Vol. 1.

63. Haber, J. A.; Lewis, N. S. Infrared and X-ray Photoelectron Spectroscopic Studies of the Reactions of Hydrogen-Terminated Crystalline Si(111) and Si(100) Surfaces with Br_2, I_2, and Ferrocenium in Alcohol Solvents. *J. Phys. Chem. B* **2002**, *106*, 3639-3656.

64. Jaeckel, B.; Hunger, R.; Webb, L. J.; Jaegermann, W.; Lewis, N. S. High-Resolution Synchrotron Photoemission Studies of the Electronic Structure and Thermal Stability of CH_3- and C_2H_5-Functionalized Si(111) Surfaces. *J. Phys. Chem. C* **2007**, *111*, 18204-18213.

65. Becker, R. S.; Golovchenko, J. A.; McRae, E. G.; Swartzentruber, B. S. Tunneling Images of Atomic Steps on the Si(111)7x7 Surface. *Phys. Rev. Lett.* **1985**, *55*, 2028-2031.

66. Yablonovitch, E.; Allara, D. L.; Chang, C. C.; Gmitter, T.; Bright, T. B. Unusually Low Surface-Recombination Velocity on Silicon and Germanium Surfaces. *Phys. Rev. Lett.* **1986**, *57*, 249-252.

67. Saadi, F. H.; Carim, A. I.; Velazquez, J. M.; Baricuatro, J. H.; McCrory, C. C. L.; Soriaga, M. P.; Lewis, N. S. Operando Synthesis of Macroporous Molybdenum Diselenide Films for Electrocatalysis of the Hydrogen-Evolution Reaction. *ACS Catalysis* **2014**, *4*, 2866-2873.

68. Roske, C. W.; Popczun, E. J.; Seger, B.; Read, C. G.; Pedersen, T.; Hansen, O.; Vesborg, P. C. K.; Brunschwig, B. S.; Schaak, R. E.; Chorkendorff, I.; Gray, H. B.; Lewis, N. S. Comparison of the Performance of CoP-Coated and Pt-Coated Radial

Junction n^+p-Silicon Microwire-Array Photocathodes for the Sunlight-Driven Reduction of Water to $H_2(g)$. *J. Phys. Chem. Lett.* **2015**, *6*, 1679-1683.

69. Callejas, J. F.; McEnaney, J. M.; Read, C. G.; Crompton, J. C.; Biacchi, A. J.; Popczun, E. J.; Gordon, T. R.; Lewis, N. S.; Schaak, R. E. Electrocatalytic and Photocatalytic Hydrogen Production from Acidic and Neutral-pH Aqueous Solutions Using Iron Phosphide Nanoparticles. *ACS Nano* **2014**, *8*, 11101-11107.
70. Sun, K.; McDowell, M. T.; Nielander, A. C.; Hu, S.; Shaner, M. R.; Yang, F.; Brunschwig, B. S.; Lewis, N. S. Stable Solar-Driven Water Oxidation to $O_2(g)$ by Ni-Oxide-Coated Silicon Photoanodes. *J. Phys. Chem. Lett.* **2015**, *6*, 592-598.
71. Sun, K.; Saadi, F. H.; Lichterman, M. F.; Hale, W. G.; Wang, H.-P.; Zhou, X.; Plymale, N. T.; Omelchenko, S. T.; He, J.-H.; Papadantonakis, K. M.; Brunschwig, B. S.; Lewis, N. S. Stable Solar-Driven Oxidation of Water by Semiconducting Photoanodes Protected by Transparent Catalytic Nickel Oxide Films. *Proc. Natl. Acad. Sci. U.S.A.* **2015**, *112*, 3612-3617.
72. Maldonado, S.; Knapp, D.; Lewis, N. S. Near-Ideal Photodiodes from Sintered Gold Nanoparticle Films on Methyl-Terminated Si(111) Surfaces. *J. Am. Chem. Soc.* **2008**, *130*, 3300-3301.
73. Maldonado, S.; Lewis, N. S. Behavior of Electrodeposited Cd and Pb Schottky Junctions on CH_3-Terminated n-Si(111) Surfaces. *J. Electrochem. Soc.* **2009**, *156*, H123-H128.
74. Fabre, B.; Lopinski, G. P.; Wayner, D. D. M. Photoelectrochemical Generation of Electronically Conducting Polymer-Based Hybrid Junctions on Modified Si(111) Surfaces. *J. Phys. Chem. B* **2003**, *107*, 14326-14335.

75. Juang, A.; Scherman, O. A.; Grubbs, R. H.; Lewis, N. S. Formation of Covalently Attached Polymer Overlayers on Si(111) Surfaces Using Ring-Opening Metathesis Polymerization Methods. *Langmuir* **2001**, *17*, 1321-1323.

76. Walter, M. G.; Liu, X.; O'Leary, L. E.; Brunschwig, B. S.; Lewis, N. S. Electrical Junction Behavior of Poly(3,4-ethylenedioxythiophene) (PEDOT) Contacts to H-Terminated and CH_3-Terminated p-, n-, and n^+-Si(111) Surfaces. *J. Phys. Chem. C* **2013**, *117*, 14485-14492.

77. Hu, S.; Shaner, M. R.; Beardslee, J. A.; Lichterman, M.; Brunschwig, B. S.; Lewis, N. S. Amorphous TiO_2 coatings stabilize Si, GaAs, and GaP photoanodes for efficient water oxidation. *Science* **2014**, *344*, 1005-1009.